



OPEN ACCESS

EDITED BY

Gerd M. Seibold,
Enzidia, Denmark

REVIEWED BY

Nils Jonathan Helmut Aversch,
University of Florida, United States
María De Los Angeles Martínez-Martínez,
Benemerita Universidad Autónoma de
Puebla, Mexico

*CORRESPONDENCE

John D. Coates
✉ jdcoates@berkeley.edu

RECEIVED 12 November 2025

REVISED 02 March 2026

ACCEPTED 09 March 2026

PUBLISHED 19 March 2026

CITATION

Meier DAO, Glazer B, Lanclos VC,
Carlson HK and Coates JD (2026)
Growth-associated polyhydroxybutyrate
accumulation in *Azospira suillum* PS
during aerobic and perchlorate
respiration.
Front. Microbiol. 17:1744475.
doi: 10.3389/fmicb.2026.1744475

COPYRIGHT

© 2026 Meier, Glazer, Lanclos, Carlson
and Coates. This is an open-access
article distributed under the terms of the
[Creative Commons Attribution License
\(CC BY\)](https://creativecommons.org/licenses/by/4.0/). The use, distribution or
reproduction in other forums is
permitted, provided the original
author(s) and the copyright owner(s) are
credited and that the original publication
in this journal is cited, in accordance
with accepted academic practice. No
use, distribution or reproduction is
permitted which does not comply with
these terms.

Growth-associated polyhydroxybutyrate accumulation in *Azospira suillum* PS during aerobic and perchlorate respiration

David A. O. Meier¹, Benjamin Glazer¹, V. Celeste Lanclos¹,
Hans K. Carlson² and John D. Coates^{1*}

¹Department of Plant and Microbial Biology, University of California, Berkeley, Berkeley, CA, United States, ²Environmental Genomics and Systems Biology Division, Lawrence Berkeley National Laboratory, Berkeley, CA, United States

Polyhydroxyalkanoates (PHAs) are widespread microbial storage polymers increasingly recognized for roles beyond carbon and energy storage, including redox homeostasis and stress physiology. While PHA accumulation is classically associated with stationary-phase metabolism under severe nutrient imbalance, comparatively little is known about growth-associated PHA synthesis in facultative anaerobes with unusual respiratory strategies. Here, we investigated polyhydroxybutyrate (PHB) metabolism in *Azospira suillum* PS, a genetically tractable perchlorate-reducing bacterium capable of both aerobic and anaerobic respiration. Using physiological growth experiments, targeted gene deletions, PHB extractions, and intracellular redox measurements, we examined PHB accumulation under varying respiratory and nutrient conditions. We demonstrate that PHB accumulates during exponential growth under moderately nitrogen-limited conditions, both aerobically and during perchlorate respiration, representing a rare example of growth-associated PHB synthesis under anaerobic conditions. Genomic analysis revealed four *phaC* homologs, one of which could not be deleted under the experimental conditions tested and co-localized with *phaB* and *phaR*. Redox profiling further revealed a strong positive correlation between PHB accumulation and intracellular NADPH/NADP⁺ ratios. Together, these findings expand the physiological contexts in which PHB synthesis is known to occur and highlight perchlorate-respiring bacteria as underexplored model systems for studying growth-integrated carbon and redox storage strategies.

KEYWORDS

Azospira suillum PS, growth associated carbon storage, metabolism, perchlorate reducing bacteria, polyhydroxybutyrate

Introduction

The use of processed polymers by humans dates to at least 1,600 B. C. E. (Hosler et al., 1999), but the invention of modern thermoplastics by Charles Goodyear in 1839 revolutionized their industrial and environmental impact. Today, thermoplastics are indispensable across nearly every sector due to their lightweight, durable, and versatile properties driving global plastic production to more than 380 million tons annually (Geyer et al., 2017). Because most

conventional plastics are derived from fossil hydrocarbons and are not biodegradable, their accumulation in the environment has intensified interest in biologically derived, degradable alternatives. Among the biodegradable alternatives under investigation, polyhydroxyalkanoates (PHAs) have attracted sustained interest because they are synthesized naturally by microorganisms from renewable carbon sources, and compostable under all ambient conditions (Rosenboom et al., 2022).

PHA is intracellular microbial polyesters that function as reserves of carbon, energy, and reducing power (Williamson and Wilkinson, 1958). Among PHAs, polyhydroxybutyrate (PHB) is the best studied, having first been identified in *Bacillus subtilis* in 1926 (Lemoigne, 1926). Although PHB was originally characterized as an inert storage compound synthesized under conditions of nutrient imbalance, PHAs are now increasingly understood as dynamic participants in microbial physiology, contributing to redox balancing, stress mitigation, and metabolic flexibility across diverse environmental contexts (Senior et al., 1972; Obruca et al., 2021; Tang et al., 2022; Sander et al., 2024). Their widespread distribution among bacteria and archaea, including organisms occupying extreme and anaerobic niches, suggests that PHAs play roles extending well beyond carbon storage during stationary phase (Emeruwa and Hawirko, 1973; Nanninga and Gottschal, 1986; Amos and McInerney, 1989; Poli et al., 2011).

In most well-characterized systems, PHB, the most common short-chain-length PHA (scl-PHA), accumulates during stationary phase in response to pronounced nutrient limitation, typically excess carbon relative to nitrogen, phosphorus, or oxygen. This paradigm has shaped both physiological and applied studies of PHB metabolism and is reinforced by work in canonical model organisms. For example, in the best-studied PHB-producing bacterium, *Cupriavidus necator*, polymer accumulation is robust but typically decoupled from exponential growth, instead requiring nutrient limitation or process-level interventions such as batch or fed-batch cultivation (Henderson and Jones, 1997; Sander et al., 2024). The prevalence of such systems has contributed to prevailing assumptions regarding PHB as a late-stage storage polymer rather than a growth-integrated metabolic process.

In contrast, growth-associated PHB accumulation, defined as polymer synthesis concurrent with exponential biomass increase, remains comparatively rare (Senior et al., 1972; Page and Knosp, 1989; Ackermann and Babel, 1997; Cristea et al., 2018; Scott et al., 2021; Woo et al., 2024). When observed, growth-associated PHB synthesis challenges the classical view of PHB as a deferred storage compound and raises fundamental questions regarding its physiological function during active growth. Recent work has expanded the known diversity of PHB-producing organisms to include anaerobes, phototrophs, syntrophs, oligotrophs, and extremophiles, demonstrating that PHB synthesis can occur across a broad range of metabolic and respiratory regimes (Dawes and Senior, 1973; Nanninga and Gottschal, 1986; Amos and McInerney, 1989; Costa et al., 2018; Wang et al., 2019; Koller and Rittmann, 2022; Bennett et al., 2024). In several of these systems, PHB has been implicated in redox homeostasis, serving as a metabolic sink for excess reducing equivalents when electron acceptor availability fluctuates or when respiratory pathways are constrained. Together, these observations support the view that PHB synthesis may be tightly coupled to intracellular redox state rather than being driven solely by nutrient limitation.

PHB biosynthesis proceeds through a conserved core pathway encoded by *phaA* (β -ketothiolase), *phaB* (acetoacetyl-CoA reductase), and *phaC* (PHA synthase), which together convert acetyl-CoA-derived intermediates into polymerized

3-hydroxybutyryl-CoA. Additional regulatory and structural proteins, including *phaR* and granule-associated *phaP* (phasin), modulate polymer accumulation, granule number, and granule morphology (Pötter et al., 2005). Based on substrate specificity and subunit composition rather than evolutionary lineage, PHA synthases (*PhaC* enzymes) are grouped into four functional classes (I–IV). Classes I, III, and IV primarily synthesize scl-PHAs such as PHB but differ in enzyme architecture: Class I enzymes function as homodimers of identical *PhaC* subunits, whereas Classes III and IV form heterodimeric complexes with accessory subunits *PhaE* and *PhaR*, respectively. In contrast, Class II PHA synthases are specialized for medium-chain-length PHAs (mcl-PHAs) and typically involve multiple *PhaC* isoforms (e.g., *PhaC1* and *PhaC2*) without accessory subunits such as *PhaE* or *PhaR*. A deeper understanding of how feedstock composition and PHA synthase structure influence polymer diversity and accumulation is needed.

Dissimilatory perchlorate-reducing bacteria (DPRB) represent a promising but understudied group in this context. Perchlorate (ClO_4^-) is a highly oxidized, water-soluble oxyanion with a biological redox potential comparable to oxygen ($E^{\circ'} = +0.797 \text{ V}$) (Youngblut et al., 2016). In DPRB, perchlorate is reduced to chlorite by the perchlorate reductase complex (*PcrAB*), followed by dismutation into chloride and molecular oxygen via chlorite dismutase (*Cld*), with the generated oxygen subsequently respired by the cell (Youngblut et al., 2016). This pathway enables endogenous O_2 generation under otherwise anoxic conditions, supporting oxygenase-dependent metabolism without external aeration (Carlström et al., 2015). The conserved and mobile perchlorate reduction island (PRI) allows this metabolism to be distributed across diverse taxa (Melnik et al., 2014). To date, the only indication that DPRB may accumulate PHB comes from a single report in *Dechloromonas agitata* CKB, where electron-dense intracellular inclusions consistent with PHA granules were observed, but without genetic or biochemical confirmation (Bruce et al., 1999).

Azospira suillum PS is a facultative anaerobe and genetically tractable perchlorate-reducing bacterium that provides a useful system for examining how PHB metabolism integrates with respiratory flexibility and intracellular redox balance. In this study, we investigate the genetic and physiological basis of PHB accumulation in *A. suillum* PS during both aerobic and perchlorate-respiring growth. By combining comparative genomics, targeted gene deletions, polymer quantification, and redox profiling, we characterize growth-associated PHB synthesis and its relationship to intracellular redox state. These findings extend emerging models of PHB as a growth-integrated, redox-coupled metabolic process to perchlorate-respiring bacteria and establish *A. suillum* PS as a model for studying the physiological role of PHB in facultative anaerobic systems.

Materials and methods

Bacterial strains and plasmids

Azospira suillum PS (ATCC BAA-33/DSMZ 13638) was revived from laboratory freezer stocks and used as the wild-type strain for all genetic manipulations. *Escherichia coli* XL1-Blue was used for plasmid propagation and cloning. A full list of primers (Supplementary Table 1), strains (Supplementary Table 2), and

plasmids (Supplementary Table 3) is provided in the Supplementary materials. Prior to all experiments, strains were streaked from freezer stocks to obtain single colonies.

Mutant construction

Gene deletion mutants in *A. suillum* PS were generated using a sacB-based counterselection approach (Gay et al., 1983). Electrocompetent cells were transformed with either integrative (~500 ng) or replicative (~50 ng) plasmids in 1 mm electroporation cuvettes using a Gene Pulser Xcell electroporator (Bio-Rad, USA) with the following settings: 1.8 kV, 25 μ F, and 200 Ω . Cells were chilled on ice before electroporation; cuvettes were kept at room temperature. After pulsing, cells were recovered in pre-warmed ALP medium at 37 °C for 6 h, then 100 μ L of culture was plated directly on ALP agar containing 50 μ g/mL kanamycin. Colonies appearing within 48 h were considered valid transformants and picked into 500 μ L ALP broth with 50 μ g/mL kanamycin. After 4 h of growth, cultures were plated on ALP agar with 6% sucrose for counterselection. Representative colonies were screened by colony PCR to confirm deletions. Glycerol stocks were prepared at 15% final concentration for storage at -80 °C.

Culture conditions and growth media

E. coli strains were cultured in LB medium with 50 μ g/mL kanamycin. Wild-type and mutant *Azospira suillum* PS strains were grown in acetate minimal medium (AMM). One liter of AMM contained: 0.49 g sodium phosphate monobasic dihydrate, 0.97 g sodium phosphate dibasic anhydrous, 0.1 g KCl, 0.25 g NH₄Cl, and 10 mL each of vitamin and mineral mix (Bruce et al., 1999). The sodium acetate concentration in AMM was either 0.82 g/L acetate for 10 mM AMM or 2.05 g acetate for 25 mM AMM. To prepare mixed carbon source media (acetate, lactate, pyruvate), AMM was supplemented with 2.0 g yeast extract, 7.6 mL of a 60% (w/w) sodium lactate solution, and 1.10 g sodium pyruvate. For solid media, 15 g/L agar was added. *A. suillum* PS was cultured in 250 mL baffled Erlenmeyer flasks containing 50 mL of medium at 37 °C and 250 rpm. Optical density at 600 nm (OD₆₀₀) was measured using a 1 mm pathlength cuvette on a Genesys 20 spectrophotometer (Thermo Scientific, USA).

PHA extraction and GC-MS analysis

PHB was quantified from 40 mL of culture. Samples were harvested by centrifugation at 7,197 \times g for 10 min at 4 °C, and pellets were stored at -80 °C. Acidic methanolysis was performed as described by Juengert et al. (2018). Extracts were analyzed by gas chromatography-mass spectrometry (GC-MS) using a 7890A GC system (Agilent Technologies, USA) equipped with a DB-WAX UI column and coupled to a 5975C XL EI/CI Mass Selective Detector. The temperature program was: 80 °C for 2 min, ramp to 210 °C at 10 °C/min, then to 250 °C at 50 °C/min with a 1 min hold. Poly[(R)-3-hydroxybutyric acid] (Santa Cruz Biotechnology, USA) was used for the standard curve, and methyl benzoate (Sigma-Aldrich, USA) served as the internal standard. Compound identity was confirmed by total ion count (TIC) spectra matching the NIST EI database. The presence of polyhydroxyvalerate (PHV) and polyhydroxyhexanoate PHHX was assessed using a commercial PHA standard (Sigma-Aldrich, USA), and TIC peaks were compared with NIST spectra for

3-hydroxypentanoic acid methyl ester and 3-hydroxyhexanoic acid methyl ester.

NAD(P)⁺/H quantification

Redox cofactor quantification was performed following the enzymatic cycling-based colorimetric assay described by Kern et al. (2014). Briefly, intracellular NAD(P)H and NAD(P)⁺ pools were differentially extracted using paired acid/base treatments to selectively destabilize oxidized versus reduced cofactors. Cell pellets were resuspended in either 0.2 M NaOH (to extract NAD(P)H) or 0.2 M HCl (to extract NAD(P)⁺), incubated at 50 °C for 10 min, neutralized with the reciprocal acid/base solution, and clarified by centrifugation.

Quantification was performed using an enzyme cycling reaction in which NAD(P)H drives reduction of phenazine ethosulfate (PES), which in turn reduces methylthiazolylidiphenyl-tetrazolium bromide (MTT). NADH was quantified using alcohol dehydrogenase and ethanol as substrate, while NADPH was quantified using glucose-6-phosphate dehydrogenase and glucose-6-phosphate. Ratios of reduced to oxidized pools were calculated from paired extracts. Samples were kept on ice and protected from light until incubated at 37 °C. To prevent redox degradation, only three samples were processed at a time. Quantification was performed using a Varian Cary 50 MPR Microplate Reader (Agilent Technologies, USA).

Fluorescence microscopy

Microscopy was conducted as described by Juengert et al. (2018). Cells were harvested in exponential phase, washed once in PBS (8 g NaCl, 201 mg KCl, 1.42 g Na₂HPO₄, 245 mg KH₂PO₄ per liter, pH 7.4), and stained with 1 μ g/mL Nile Red for 10 min in the dark. Samples were mounted on 1% agarose pads and visualized on a Zeiss LSM880 confocal microscope (Zeiss, Germany) using a 100 \times Plan-Apochromat NA 1.4 objective. Nile Red was excited at 561 nm, and emission was detected from 570–620 nm using a GaAsP photon-counting detector. Differential interference contrast (DIC) images were acquired simultaneously. Image acquisition settings were consistent across all samples and processed in ZEN software v2.3 SP1 (Zeiss).

Phylogenetic tree construction

Each *phaC* gene from *A. suillum* PS was queried against the NCBI nr database using BLASTP (Altschul et al., 1990). The top 250 unique hits (excluding “multispecies” entries) were retained per gene. PhaC homologs from *Azospira* species were manually reviewed and validated using HMMER v3.4 with TIGRfam-specific models (Finn et al., 2011). Alignments were generated with MUSCLE v3.8.31 and trimmed using trimAl v1.4 (Edgar, 2004; Capella-Gutiérrez et al., 2009). Phylogenies were inferred using IQ-TREE v2.0.6 with 1,000 ultrafast bootstraps and the Q.pfam+I + R7 model. Trees were visualized using iTOL v6 (Minh et al., 2020; Letunic and Bork, 2021).

In silico comparative genomics

The genome of *A. suillum* PS was downloaded from NCBI (Sayers et al., 2024); *D. agitata* CKB and additional *Azospira* genomes were retrieved from JGI-IMG (Markowitz et al., 2006). Genomes were searched using HMMER v3.4 with a custom set of TIGRfams relevant

to PHA metabolism (Supplementary Table 4). Presence/absence patterns of PHA biosynthesis genes were visualized using R v4.4.2 and RStudio v2024.12.0 + 467.

Results

Genomic and microscopic evidence for PHB granule formation in *A. suillum* PS and other perchlorate-reducing bacteria

Comparative genomic analysis of perchlorate-reducing bacteria revealed that both *D. agitata* CKB and *A. suillum* PS encode the complete set of genes required for PHA biosynthesis, including, *phaC*, and *phaR* (Figure 1C). Both genomes contain multiple *phaC* homologs, with three copies in CKB and four in PS, one of which in each organism is co-localized with *phaB* and *phaR* in an apparent operon arrangement. The remaining *phaC* copies are distributed elsewhere in the genome; only one is located adjacent to a *phaP* gene, and no additional cluster-level organization associated with PHA biosynthesis was observed. These genomic features motivated the selection of *A. suillum* PS as a genetically tractable system for experimentally characterizing PHA production under aerobic and perchlorate-respiring conditions.

To determine whether *A. suillum* PS produced PHB granules, we stained cultured cells with Nile Red, a lipophilic dye commonly used to visualize PHB granules and examined them using confocal microscopy (Figure 1B). Distinct intracellular lipid inclusions consistent with PHB granules were observed, with an approximate diameter of 0.32 μm. Given

the ~2 μm cell diameter of PS, the clustered granules span much of the intracellular space, corresponding to ~64% of the estimated cell volume being occupied by PHB granules. Cells stained positive for PHB granules under both aerobic and perchlorate-respiring conditions, providing the first clear evidence of PHA production linked to perchlorate respiration. This observation confirmed the genetic potential for PHB accumulation; however, it remained unclear whether polymer synthesis occurred constitutively or only in response to specific nutrient conditions.

To establish whether PHB accumulation in *A. suillum* PS is constitutive or nutrient-dependent, we first evaluated growth under nitrogen-replete conditions. Cultures were grown in standard acetate minimal medium (AMM) containing 10 mM sodium acetate and 4.68 mM NH₄Cl, corresponding to a replete C:N ratio of approximately 1:0.23 relative to the canonical Redfield ratio (C:N = 1:0.15) (Redfield, 1934). Under these conditions, no detectable PHB was observed by GC-MS analysis (Figure 1D), confirming that PHB synthesis does not occur under nitrogen-replete growth. The culture exhibited a specific growth rate (μ) of 0.60 h⁻¹ and a doubling time of 1.16 h, indicating robust biomass formation despite the absence of polymer accumulation. Although the final optical density under nitrogen-replete conditions (Figure 1) was lower than in carbon-enriched, nitrogen-limited cultures (Figure 2), this difference reflects the smaller amount of carbon supplied (10 mM vs. 25 mM acetate) rather than reduced growth capability. Consistent with this, the higher OD observed under the C:N = 1:0.094 condition results from increased carbon availability, not enhanced growth efficiency, as shown by the lower specific growth rate measured in that condition.

Given prior genomic and microscopic evidence suggesting PHB-producing potential, we next examined whether altering the carbon-to-nitrogen ratio could induce polymer synthesis. When the acetate concentration was increased to 25 mM while maintaining 4.68 mM

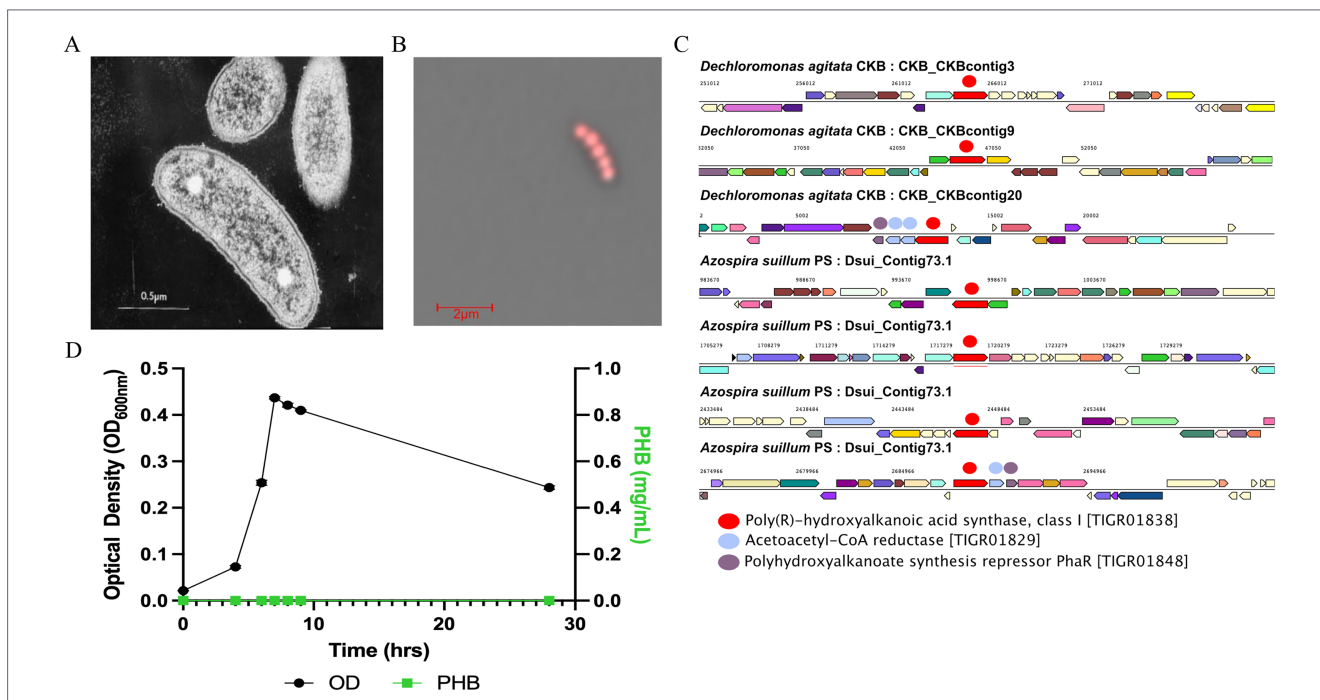
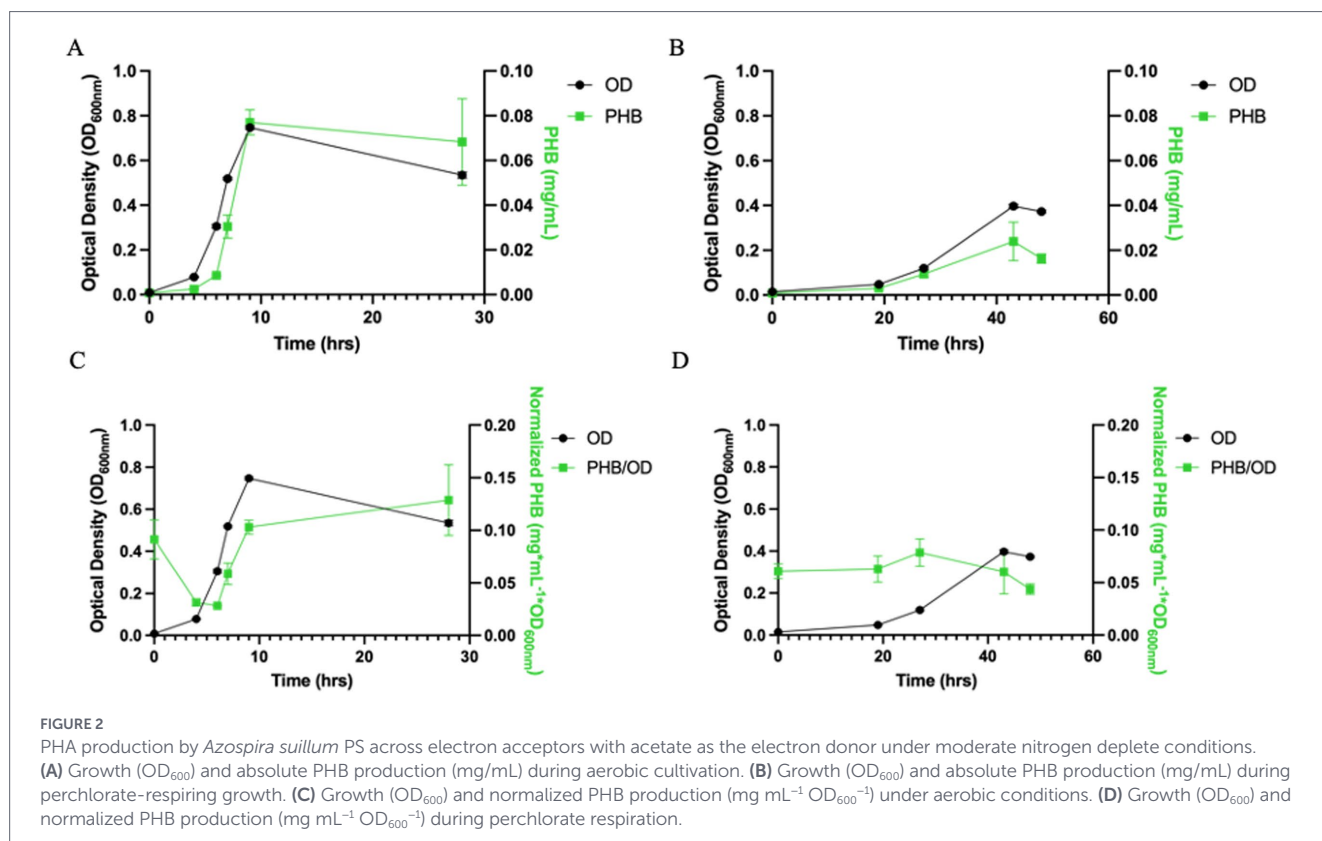


FIGURE 1 Microscopic and comparative genomic analysis of PHA production in *Dechloromonas agitata* CKB and *Azospira suillum* PS. (A) Transmission electron micrograph (TEM) of *D. agitata* CKB adapted from Bruce et al. (1999), showing electron-dense inclusions consistent with PHA granules. (B) Confocal fluorescence microscopy image of Nile Red-stained *A. suillum* PS grown under perchlorate-respiring conditions, overlaid with transmitted light, highlighting intracellular PHA granules. (C) Gene neighborhood analysis of *phaC* loci in CKB and PS, with neighboring PHA biosynthesis genes highlighted where present in the red box. (D) Growth (OD₆₀₀) and absolute PHB production (mg/mL) by *A. suillum* PS during aerobic cultivation under nitrogen replete growth conditions.



NH_4Cl (C:N = 1:0.094), PHB production was observed under both aerobic and perchlorate-respiring conditions (Figures 2A–D). Under these carbon-enriched conditions, cell experience ~38% less nitrogen per unit carbon than under the canonical Redfield ratio, experiencing moderate nitrogen limitation. Under these conditions *A. suillum* PS exhibited a slightly reduced specific growth rate ($\mu = 0.50\ h^{-1}$; doubling time = 1.39 h) but accumulated measurable intracellular PHB. These results demonstrate that PHB synthesis in *A. suillum* PS is triggered by a shift toward carbon surplus relative to nitrogen, rather than being a constitutive feature of its metabolism.

Following this finding, we conducted a detailed time-course analysis of PHB accumulation under the carbon-enriched condition to quantify the extent and dynamics of polymer synthesis during aerobic and perchlorate-respiring growth.

Growth-associated PHB production in *Azospira suillum* PS under aerobic and perchlorate-respiring conditions

To quantify PHA production by *A. suillum* PS, GC–MS was performed on samples extracted via acidic methanolysis. In addition to quantifying total PHB produced by the culture, this method also enabled identification of the different monomers present. When PS was grown on acetate under either aerobic or perchlorate-respiring conditions 3-hydroxybutyric acid (3-HB) (the monomer of PHB) was detected. PHB was quantified across the growth curve and was found to be produced in a growth-associated manner (Figures 2A–D).

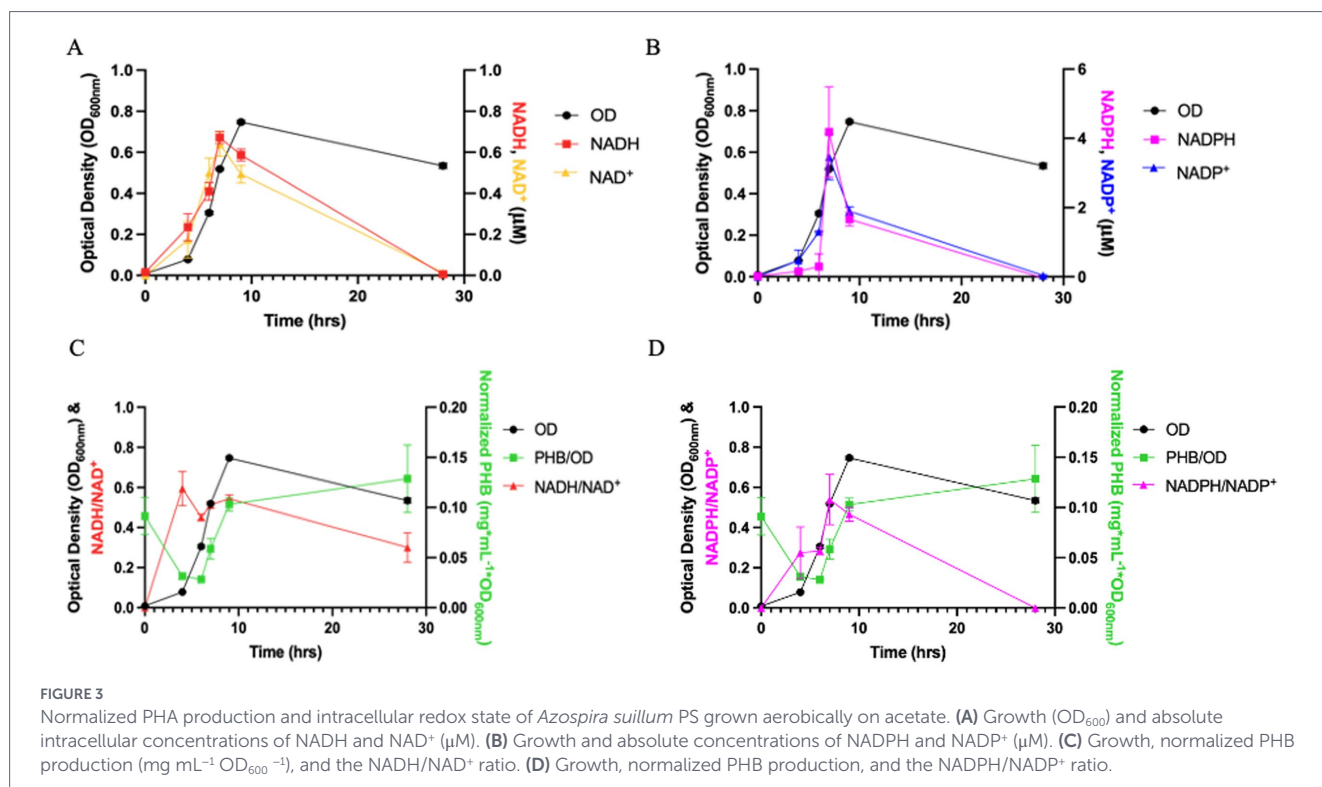
When grown aerobically, *A. suillum* PS reaches a maximum OD_{600nm} of 0.747 ± 0.008 during late exponential phase, at which point it had produced a maximum of $0.077 \pm 0.006\ mg/mL$ PHB providing a total yield of $0.10\ g/L$ per OD_{600nm} (Figure 2A). Under

perchlorate-respiring conditions with 10 mM perchlorate, PS reaches a lower maximum OD_{600nm} of 0.397 ± 0.009 and produces a maximum of $0.024 \pm 0.008\ mg/mL$ PHB or $0.06\ g/L$ per OD_{600nm} (Figure 2B). When grown on perchlorate, PHB levels slightly decline as the culture enters stationary phase (Figure 2D). There is no significant reduction in PHB levels between peak and late-stage culture under aerobic conditions, despite a drop in OD_{600nm} of approximately 0.21. Based on the 1.6-fold higher PHB yield in aerobic versus perchlorate conditions, we further characterized PHB production by PS under aerobic growth. This growth-associated pattern under carbon-enriched conditions contrasts with the nitrogen-replete culture, where no PHB was detected, reinforcing that polymer synthesis in *A. suillum* PS is activated only when the C:N ratio exceeds a physiological threshold.

When examining normalized PHB levels relative to optical density, both aerobic and perchlorate-grown cultures show evidence of carry-over PHB from the inoculum (Figures 2C,D). In aerobic cultures, this residual PHB is rapidly degraded during lag phase prior to new PHB accumulation during log phase, suggesting that the cells may utilize the carryover PHB as an additional electron donor alongside the supplied acetate during the initial phase of growth (Figure 2C). In contrast, perchlorate-respiring cultures do not exhibit this initial degradation phase; instead, normalized PHB/ OD_{600} remains stable during early growth and begins increasing only during exponential phase.

Redox cofactor dynamics link NADPH availability to PHB biosynthesis in *Azospira suillum* PS

To assess the redox influence on PHB biosynthesis, we measured intracellular NADH/NAD⁺ and NADPH/NADP⁺ ratios over a 24-h



culture period and compared these values to PHB accumulation (Figures 3A–D). When grown aerobically, *Azospira suillum* PS exhibited an average NADH/ NAD^+ ratio of 0.491—more than twice the reported aerobic values for *E. coli* (0.226) and *Klebsiella aerogenes* (0.195) (Wimpenny and Firth, 1972)—indicating a relatively reduced intracellular environment.

Spearman correlation analysis revealed a strong and statistically significant monotonic relationship between PHB levels and NADPH/ $NADP^+$ ($\rho = 0.829$, $p = 0.042$), while no significant correlation was observed with NADH/ NAD^+ ($\rho = 0.600$, $p = 0.208$). This is consistent with the known cofactor specificity of the PhaB acetoacetyl-CoA reductase enzyme. In *Cupriavidus necator* H16—a well-studied model organism for PHB production—this enzyme has been shown to preferentially use NADPH rather than NADH as the reducing equivalent source (Steinbüchel and Schlegel, 1991).

Phylogenomic analysis reveals conserved, diversified *phaC* loci across the *Azospira* genus

A maximum-likelihood phylogenetic tree (Figure 4) constructed from the four unique *phaC* gene products identified in *Azospira suillum* PS, along with their 250 closest homologs, revealed that each PhaC protein is nested within a monophyletic clade composed of *phaC* homologs from other *Azospira* species. Despite this shared genus-level affiliation, the four *phaC* variants from strain PS occupy distinct and divergent branches within the tree, suggesting that each *phaC* gene may have evolved independently. Furthermore, this analysis revealed that multiple *phaC* gene copies are consistently present in *Azospira* genomes. Comparative genomic analysis across the genus showed that each *Azospira* species encodes at least three distinct copies of *phaC*, alongside a single copy of the transcriptional regulator *phaR*, suggesting that PHA biosynthesis is a conserved metabolic feature within the genus (Figure 5). To assess

whether these genes may have been acquired via horizontal gene transfer, we used IslandViewer (Bertelli et al., 2017), which predicts genomic islands based on sequence composition and comparative genomics. This analysis showed no evidence of horizontal gene transfer near the *phaC* loci in strain PS (data not shown).

To assess conservation of gene neighborhoods, we used CAGE-CAT and Clinker to compare the genomic loci surrounding *phaC* across *Azospira* genomes (Gilchrist and Chooi, 2021). These tools align and visualize syntenic regions based on protein sequence identity and gene order, enabling rapid identification of conserved operons and structural rearrangements. This analysis (Figure 6) revealed that the local gene context of *phaC* is highly conserved, with pairwise amino acid identity of *phaC* homologs exceeding 70% across the genus, further supporting their functional importance in *Azospira*. However, while average nucleotide identity remains high across *Azospira* species, they do not share syntenic conservation of the broader PHA biosynthesis gene cluster.

Functional characterization of *phaC* genes identifies *phaC4* as non-deletable under tested conditions

Our analysis found that *Azospira suillum* PS encodes only class I *phaC* genes, which are typically associated with the production of scl-PHAs such as PHB. To investigate the four *phaC* genes in *A. suillum* PS responsible for PHA production, we attempted to generate deletion mutants for each gene. Knockout strains were successfully constructed for three out of the four *phaC* genes. However, under all tested growth conditions, we were unable to generate a mutant lacking the *phaC* gene with the locus tag *dsui_2537* (*phaC4*). Notably, this gene is colocalized with *phaB* and *phaR*. Previous transposon mutagenesis studies in strain PS also identified *phaC4* as conditionally essential under all conditions tested (Supplementary Figure 1).

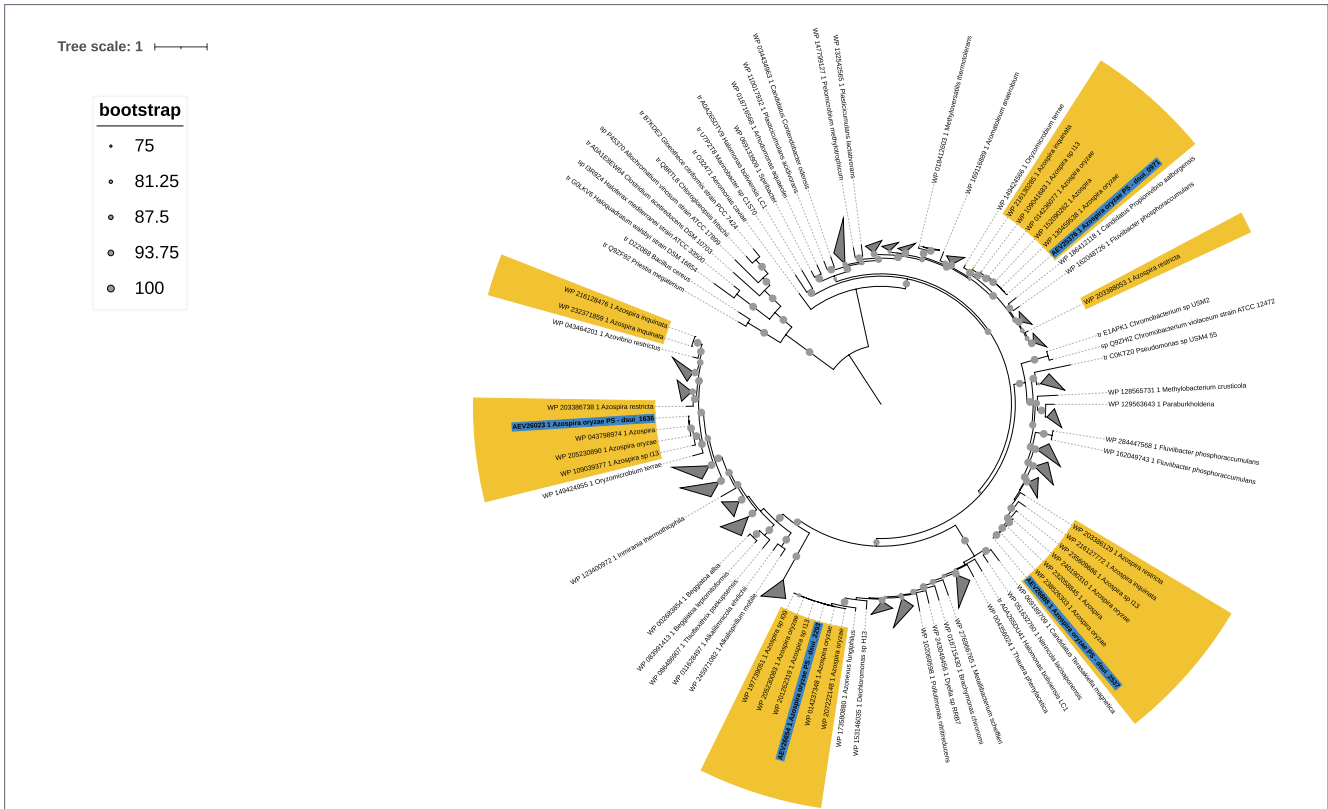


FIGURE 4
PhaC protein phylogeny within the genus *Azospira*. Maximum likelihood phylogenetic tree of PhaC protein sequences from members of the genus *Azospira*. Bootstrap support values ($n = 1,000$ replicates) are shown at each node. Branches corresponding to *Azospira* species are highlighted in yellow, and those from *A. suillum* PS are further annotated in green. Tip labels include the GenBank protein accession number followed by the corresponding NCBI organism name.

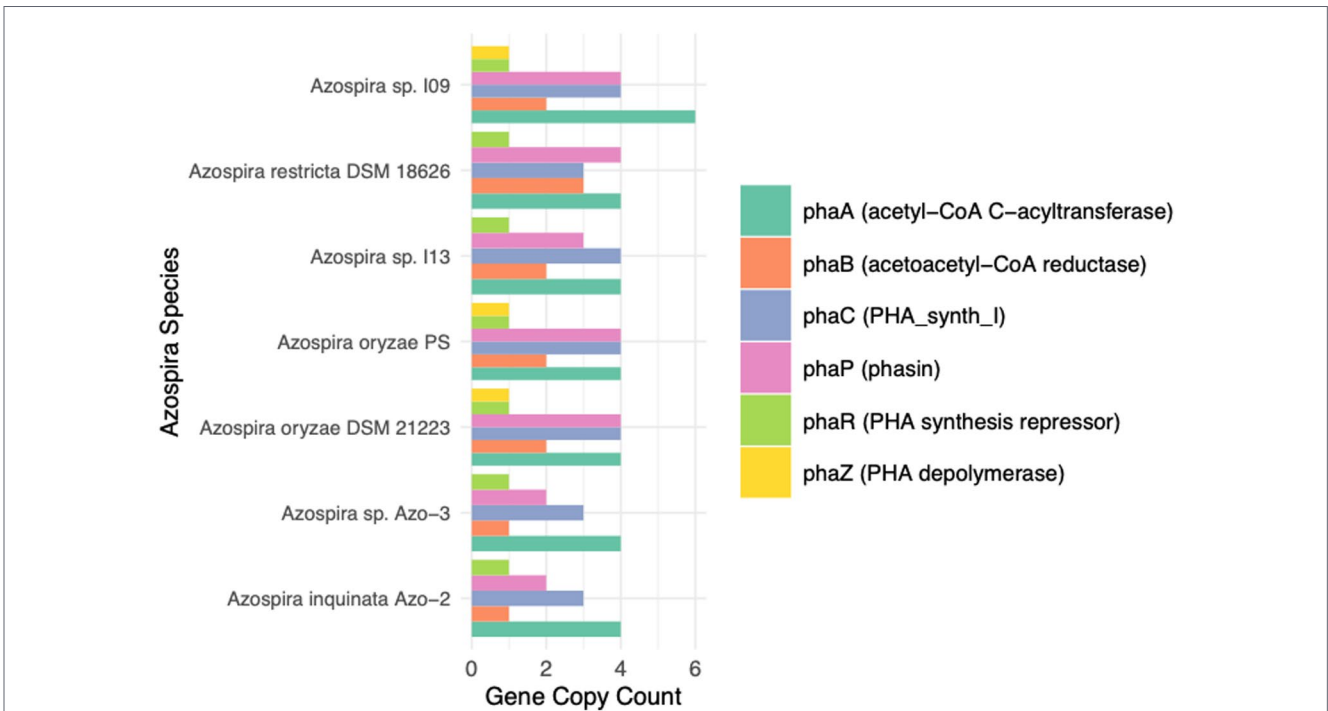


FIGURE 5
Stacked barplot showing the copy number of PHA-associated gene families identified in each available *Azospira* genome. Each bar represents a genome, and colored segments correspond to individual gene families detected by HMMER above noise cutoff thresholds. Values indicate total gene counts per family within each genome.

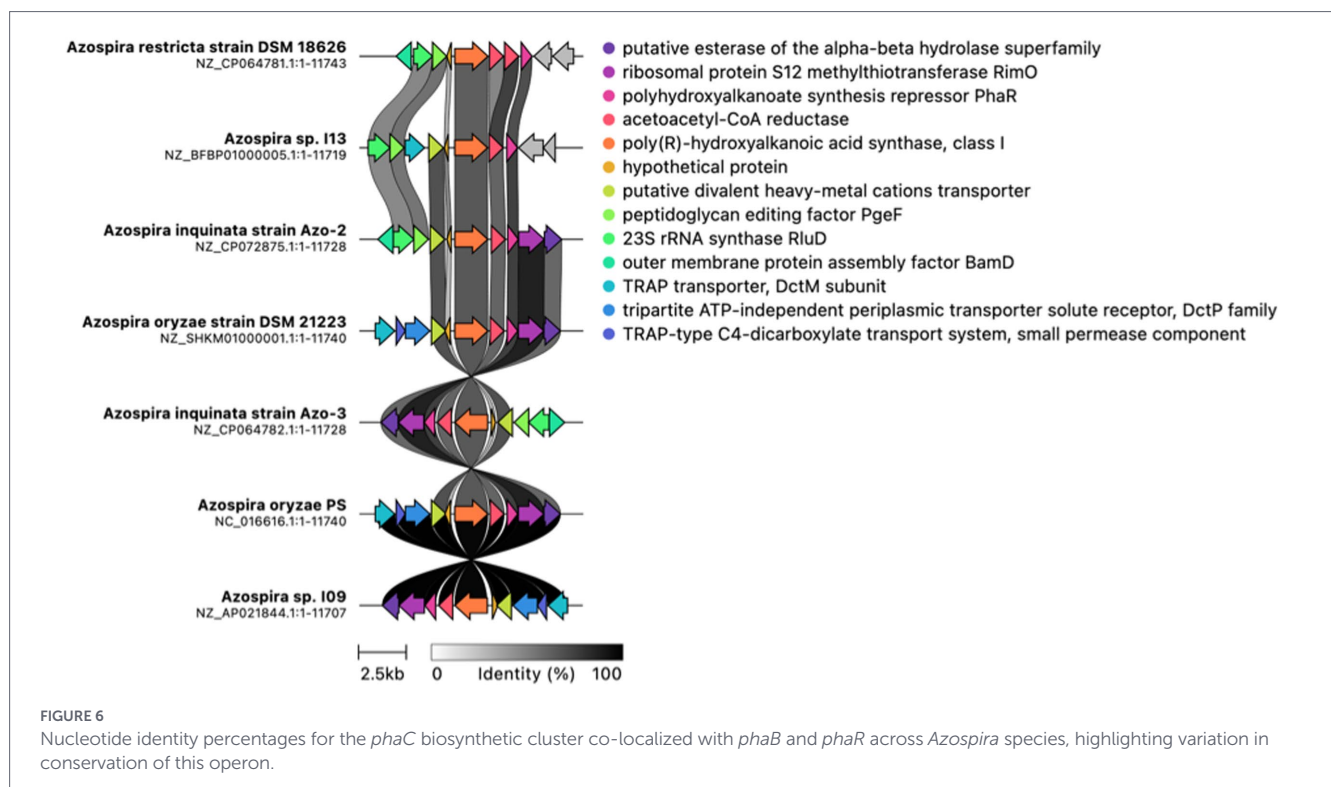


TABLE 1 Polyhydroxyalkanoate methyl esters produced by *Azospira suillum* PS when grown on complex or defined media.

| Strains | PHB | PHV | PHHX |
|-----------------------------|-----|-----|------|
| WT | + | - | - |
| $\Delta phaC1$ | + | - | - |
| $\Delta phaC2$ | + | - | - |
| $\Delta phaC3$ | + | - | - |
| $\Delta(phaC1-phaC2)$ | + | - | - |
| $\Delta(phaC1-phaC3)$ | + | - | - |
| $\Delta(phaC2-phaC3)$ | + | - | - |
| $\Delta(phaC1-phaC2-phaC3)$ | + | - | - |

Summary of PHA monomers identified in *A. suillum* PS when cultivated on complex media (acetate, lactate, pyruvate with yeast extract) or defined acetate minimal medium. PS locus tags corresponding to each *phaC* gene are listed in Supplementary Table 5.

To further assess the functional role of each *phaC*, we compared the PHA monomer profiles of all knockout strains under both defined and complex media conditions. As shown in Table 1, none of the knockout strains displayed a PHA profile distinct from wild type. All strains consistently produced PHB, while PHV and PHHX were absent (data not shown). These results suggest that the conditionally essential *phaC4* is playing an important physiological role during normal growth in nutrient replete media.

Discussion

The central finding of this study is that PHB synthesis in *Azospira suillum* PS is growth-associated and occurs under moderate nitrogen limitation during both aerobic and perchlorate-respiring metabolism.

Rather than accumulating as a late-stage storage polymer following growth arrest, PHB in PS is synthesized concurrently with biomass increase and remains quantitatively modest. This pattern suggests that PHB functions as a dynamic metabolic intermediate integrated into central metabolism rather than as a long-term carbon reserve.

The induction of PHB exclusively under carbon-enriched conditions indicates that polymer synthesis in PS is regulated by C:N imbalance rather than constitutive expression. Notably, increasing the severity of nitrogen limitation did not further enhance PHB accumulation, suggesting that once a carbon-surplus threshold is reached, additional nitrogen restriction does not proportionally stimulate polymer production. A similar pattern has been observed in other anaerobic organisms, including *Syntrophomonas wolfei*, in which PHB synthesis occurred independently of ammonium chloride concentration (Amos and McInerney, 1989). Importantly, PHB accumulation was observed under both oxygen-respiring and perchlorate-respiring conditions, indicating that this regulatory architecture is independent of terminal electron acceptor identity. This respiratory-mode agnosticism supports the interpretation that PHB flux in PS is more closely linked to intracellular redox balance and carbon partitioning than to the specific respiratory pathway in use.

Growth-associated PHB synthesis has been reported in a limited number of systems (Senior et al., 1972; Page and Knosp, 1989; Ackermann and Babel, 1997; Cristea et al., 2018; Scott et al., 2021; Woo et al., 2024), yet it remains comparatively uncommon relative to the classical paradigm in which PHB accumulates predominantly during stationary phase under pronounced nutrient imbalance (Anderson and Dawes, 1990; Sander et al., 2024). The phenotype observed in *A. suillum* PS therefore aligns with a smaller but growing body of literature suggesting that PHB can function as a growth-integrated metabolic sink rather than solely as a late-stage storage polymer.

Temporal analysis revealed distinct regulatory patterns between respiratory modes. Under aerobic growth, normalized PHB/OD₆₀₀

declined during lag phase, likely reflecting mobilization of stored carbon and reducing equivalents inherited from the inoculum, followed by renewed PHB accumulation during exponential growth. In contrast, perchlorate-respiring cultures did not exhibit this early degradation phase; PHB levels remained stable during early growth and increased only during exponential phase.

Using established correlations between OD₆₀₀ and cell dry weight for morphologically similar organisms (Glazyrina et al., 2010), the maximum aerobic PHB concentration in *Azospira suillum* PS corresponds to approximately 2.6–3.2% PHB per CDW, while perchlorate-respiring cultures accumulated approximately 1.5–2.5% PHB per CDW. Thus, PS accumulates measurable PHB under both respiratory modes, with aerobic growth supporting ~1.6-fold greater PHB per unit biomass. These modest PHB fractions stand in marked contrast to the large stationary-phase PHB reserves characteristic of classical storage organisms such as *Cupriavidus necator*, which can accumulate 60–80% CDW PHB under severe nutrient imbalance (Zhang et al., 2022). In PS, however, PHB is synthesized exclusively during active growth and remains quantitatively small, supporting the interpretation that this organism utilizes PHB as a dynamic metabolic intermediate rather than a long-term carbon store.

These PHB fractions fall within the quantitative range reported for other anaerobic microorganisms exhibiting growth-associated or redox-linked PHB accumulation, such as *Syntrophomonas wolfei* (~35 µg mL⁻¹ PHB) (Amos and McInerney, 1989). However, they are lower than the PHB levels reported for moderately accumulating fermentative organisms such as *Clostridium botulinum* (9–13% CDW) (Emeruwa and Hawirko, 1973), and substantially below the large PHB reserves observed in strongly carbon-imbalanced anaerobes, including sulfate-reducing bacteria (20–43% CDW) (Hai et al., 2004). Comparable low-to-moderate PHB fractions have also been reported for some halophilic archaea, where PHB content spans a broad range (0.05–63% CDW) depending on species and carbon source (Poli et al., 2011).

The distinction between PS and *C. necator* is therefore not merely quantitative but fundamentally physiological. Whereas *C. necator* accumulates extraordinarily high PHB fractions only after entering stationary phase and only under severe nutrient imbalance, PS produces small but consistent quantities of PHB throughout exponential growth under both aerobic and perchlorate-respiring conditions. This growth-associated phenotype which is agnostic of respiratory-mode suggests a regulatory role for PHB linked to central metabolism and electron balance rather than carbon storage.

A strong and statistically significant correlation was observed between intracellular NADPH/NADP⁺ ratios and PHB content (Spearman $\rho = 0.829$, $p = 0.042$), implicating NADPH availability as a potential driver of PHB accumulation. Although this correlation suggests a role for NADPH in fueling PHB biosynthesis, it does not establish direct cofactor specificity of the biosynthetic enzymes. NADH and NADPH pools are often tightly coupled and metabolically interconvertible, and the observed association may therefore reflect broader intracellular redox state rather than exclusive NADPH usage. Nevertheless, this relationship is consistent with the known NADPH preference of PhaB acetoacetyl-CoA reductases in other organisms (Steinbüchel and Schlegel, 1991; Ling et al., 2018). Further biochemical characterization will be required to determine whether PhaB or related enzymes in PS preferentially utilize NADPH over

NADH and to define how NADPH-generating reactions interface with PHB flux.

The elevated NADH/NAD⁺ ratios observed during aerobic growth in PS further support a relatively reduced intracellular environment compared to several well-characterized facultative bacteria (Wimpenny and Firth, 1972). Only respiratory generalists such as *Pseudomonas aeruginosa* have been reported to exhibit similarly high aerobic NADH/NAD⁺ ratios. While *Escherichia coli* lacks native PHA biosynthetic capacity, certain *Pseudomonas* species are capable of PHB production, although typically not in a growth-associated manner (Bertrand et al., 1990). The comparatively reduced redox state of PS may therefore create metabolic conditions that favor diversion of carbon flux into PHB as a mechanism for dissipating excess reducing equivalents.

Genomic analysis revealed four *phaC* genes encoding class I PHA synthases in *A. suillum* PS. Among these, *phaC4* is notable for its synteny with *phaB* and *phaR*, consistent with a conserved operon structure. No evidence of horizontal gene transfer was detected near any *phaC* locus, indicating that these genes are native and vertically inherited. Repeated attempts to generate a deletion mutant of *phaC4* were unsuccessful under all growth conditions tested, whereas deletion mutants were readily obtained for the other three *phaC* genes. Independent random barcode transposon mutagenesis data in strain PS also failed to recover insertions in *phaC4* (Supplementary Figure 1), demonstrating conditional essentiality under all conditions tested. Together, these findings indicate that PHB biosynthesis is deeply integrated into the core physiology of PS, potentially functioning as a mechanism for maintaining intracellular redox balance rather than serving solely as a dispensable storage pathway.

By combining genomic analysis, targeted gene deletions, polymer quantification, and redox profiling, this study establishes *Azospira suillum* PS as the first isolated perchlorate-reducing bacterium demonstrated to synthesize PHB and as a mechanistically tractable model for studying growth-integrated, redox-coupled PHB metabolism in facultative anaerobes. PHB synthesis was absent under nitrogen-replete conditions and was induced only when the carbon-to-nitrogen ratio was altered to impose an approximately 40% reduction in nitrogen availability relative to the canonical Redfield ratio, demonstrating that polymer accumulation is triggered by moderate nutrient imbalance rather than severe starvation. The induction of PHB exclusively under carbon-surplus conditions is consistent with classical C:N-governed regulation of PHB biosynthesis (Sander et al., 2024), while the strong linkage observed here between PHB accumulation, intracellular NADPH/NADP⁺ ratios, and *phaC* operon organization supports a model in which PHB flux is integrated with central redox metabolism.

Beyond defining a new physiological phenotype in perchlorate-respiring bacteria, these findings broaden the recognized metabolic contexts for PHA production and underscore the importance of examining PHB biosynthesis within its native metabolic and ecological framework. The growth-associated synthesis observed under both perchlorate-respiring and aerobic conditions provides a foundation for future biochemical and genetic studies aimed at dissecting regulatory control, enzyme specificity, and flux partitioning, and may inform exploration of redox-balanced or continuous cultivation strategies. However, such efforts will ultimately depend on a deeper mechanistic understanding of how NADPH metabolism, *phaC* paralogs function, and redox homeostasis collectively govern PHB flux in this system.

Data availability statement

The datasets presented in this study can be found in online repositories. The names of the repository/repositories and accession number(s) can be found in the article/[Supplementary material](#).

Author contributions

DM: Data curation, Formal analysis, Investigation, Methodology, Writing – original draft. BG: Investigation, Methodology, Validation, Writing – review & editing. VL: Investigation, Methodology, Writing – review & editing. HC: Conceptualization, Methodology, Resources, Writing – review & editing. JC: Conceptualization, Funding acquisition, Investigation, Methodology, Project administration, Resources, Supervision, Writing – review & editing.

Funding

The author(s) declared that financial support was received for this work and/or its publication. This research was supported in part by generous sponsorship from the American Pacific Corporation and the Baydin (Boomerang) Corporation.

Acknowledgments

The authors acknowledge Yi Liu for guidance on instrumentation and analyses, Denise Schichnes at the UC Berkeley Biological Imaging Facility for training and access to microscopy, and Ruiwen Hu for his advice on computational analyses.

References

- Ackermann, J.-U., and Babel, W. (1997). Growth-associated synthesis of poly(hydroxybutyric acid) in *Methylobacterium rhodesianum* as an expression of an internal bottleneck. *Appl. Microbiol. Biotechnol.* 47, 144–149. doi: 10.1007/s002530050903
- Altschul, S. F., Gish, W., Miller, W., Myers, E. W., and Lipman, D. J. (1990). Basic local alignment search tool. *J. Mol. Biol.* 215, 403–410. doi: 10.1016/S0022-2836(05)80360-2
- Amos, D. A., and McInerney, M. J. (1989). Poly- β -hydroxyalkanoate in *Syntrophomonas wolfei*. *Arch. Microbiol.* 152, 172–177. doi: 10.1007/BF00456097
- Anderson, A. J., and Dawes, E. A. (1990). Occurrence, metabolism, metabolic role, and industrial uses of bacterial Polyhydroxyalkanoates. *Microbiol. Rev.* 54, 450–472. doi: 10.1128/mr.54.4.450-472.1990
- Bennett, B. D., Meier, D. A. O., Lanclos, V. C., Asrari, H., Coates, J. D., and Thrash, J. C. (2024). Polyhydroxybutyrate production in freshwater SAR11 (LD12). *Microbiology*. 19. doi: 10.1101/2024.11.08.622676
- Bertelli, C., Laird, M. R., Williams, K. P., Simon Fraser University Research Computing Group, Lau, B. Y., Hoad, G., et al. (2017). IslandViewer 4: expanded prediction of Genomic Islands for larger-scale datasets. *Nucleic Acids Res.* 45, W30–W35. doi: 10.1093/nar/gkx343
- Bertrand, J.-L., Ramsay, B. A., Ramsay, J. A., and Chavarie, C. (1990). Biosynthesis of poly- β -Hydroxyalkanoates from Pentoses by *Pseudomonas Pseudoflava*. *Appl. Environ. Microbiol.* 56, 3133–3138. doi: 10.1128/aem.56.10.3133-3138.1990
- Bruce, R. A., Achenbach, L. A., and Coates, J. D. (1999). Reduction of (per)chlorate by a novel organism isolated from paper mill waste. *Environ. Microbiol.* 1, 319–329. doi: 10.1046/j.1462-2920.1999.00042.x
- Capella-Gutiérrez, S., Silla-Martínez, J. M., and Gabaldón, T. (2009). trimAl: a tool for automated alignment trimming in large-scale phylogenetic analyses. *Bioinf. (Oxf.)* 25, 1972–1973. doi: 10.1093/bioinformatics/btp348
- Carlström, C. I., Loutey, D., Bauer, S., Clark, I. C., Rohde, R. A., Iavarone, A. T., et al. (2015). (per)chlorate-reducing bacteria can utilize aerobic and anaerobic pathways of aromatic degradation with (per)chlorate as an electron acceptor. *mBio* 6:e02287-14. doi: 10.1128/mBio.02287-14
- Costa, S. S., Miranda, A. L., Andrade, B. B., Assis, D. d. J., Souza, C. O., de Moraes, M. G., et al. (2018). Influence of nitrogen on growth, biomass composition, production, and properties of Polyhydroxyalkanoates (PHAs) by microalgae. *Int. J. Biol. Macromol.* 116, 552–562. doi: 10.1016/j.ijbiomac.2018.05.064
- Cristea, A., Baricz, A., Leopold, N., Floare, C. G., Borodi, G., Kacso, I., et al. (2018). Polyhydroxybutyrate production by an extremely halotolerant *Halomonas Elongata* strain isolated from the hypersaline meromictic Fără fund Lake (Transylvanian Basin, Romania). *J. Appl. Microbiol.* 125, 1343–1357. doi: 10.1111/jam.14029
- Dawes, E. A., and Senior, P. J. (1973). The role and regulation of energy reserve polymers in micro-organisms. *Adv Microb Physiol* 10, 135–266. doi: 10.1016/s0065-2911(08)60088-0
- Edgar, R. C. (2004). MUSCLE: multiple sequence alignment with high accuracy and high throughput. *Nucleic Acids Res.* 32, 1792–1797. doi: 10.1093/nar/gkh340
- Emeruwa, A. C., and Hawirko, R. Z. (1973). Poly- β -Hydroxybutyrate metabolism during growth and sporulation of *Clostridium botulinum*. *J. Bacteriol.* 116, 989–993. doi: 10.1128/jb.116.2.989-993.1973
- Finn, R. D., Clements, J., and Eddy, S. R. (2011). HMMER web server: interactive sequence similarity searching. *Nucleic Acids Res.* 39, W29–W37. doi: 10.1093/nar/gkr367

Conflict of interest

The author(s) declared that this work was conducted in the absence of any commercial or financial relationships that could be construed as a potential conflict of interest.

Generative AI statement

The author(s) declared that Generative AI was not used in the creation of this manuscript.

Any alternative text (alt text) provided alongside figures in this article has been generated by Frontiers with the support of artificial intelligence and reasonable efforts have been made to ensure accuracy, including review by the authors wherever possible. If you identify any issues, please contact us.

Publisher's note

All claims expressed in this article are solely those of the authors and do not necessarily represent those of their affiliated organizations, or those of the publisher, the editors and the reviewers. Any product that may be evaluated in this article, or claim that may be made by its manufacturer, is not guaranteed or endorsed by the publisher.

Supplementary material

The Supplementary material for this article can be found online at: <https://www.frontiersin.org/articles/10.3389/fmicb.2026.1744475/full#supplementary-material>

- Gay, P., Le Coq, D., Steinmetz, M., Ferrari, E., and Hoch, J. A. (1983). Cloning structural Gene sacB, which codes for exoenzyme Levansucrase of *Bacillus Subtilis*: expression of the Gene in *Escherichia Coli*. *J. Bacteriol.* 153, 1424–1431. doi: 10.1128/jb.153.3.1424-1431.1983
- Geyer, R., Jambeck, J. R., and Law, K. L. (2017). Production, use, and fate of all plastics ever made. *Sci. Adv.* 3:e1700782. doi: 10.1126/sciadv.1700782
- Gilchrist, C. L. M., and Chooi, Y.-H. (2021). Clinker & clustermap.js: automatic generation of gene cluster comparison figures. *Bioinformatics* 37, 2473–2475. doi: 10.1093/bioinformatics/btab007
- Glazyrina, J., Materne, E.-M., Dreher, T., Storm, D., Junne, S., Adams, T., et al. (2010). High cell density cultivation and recombinant protein production with *Escherichia coli* in a rocking-motion-type bioreactor. *Microb. Cell Factories* 9:42. doi: 10.1186/1475-2859-9-42
- Hai, T., Lange, D., Rabus, R., and Steinbüchel, A. (2004). Polyhydroxyalkanoate (PHA) accumulation in sulfate-reducing bacteria and identification of a class III PHA synthase (PhaEC) in *Desulfococcus Multivorans*. *Appl. Environ. Microbiol.* 70, 4440–4448. doi: 10.1128/AEM.70.8.4440-4448.2004
- Henderson, R. A., and Jones, C. W. (1997). Physiology of Poly-3-Hydroxybutyrate (PHB) production by *Alcaligenes Eutrophus* growing in continuous culture. *Microbiology* 143, 2361–2371. doi: 10.1099/00221287-143-7-2361
- Hosler, D., Burkett, S. L., and Tarkanian, M. J. (1999). Prehistoric polymers: rubber processing in ancient Mesoamerica. *Science* 284, 1988–1991. doi: 10.1126/science.284.5422.1988
- Juengert, J., Bresan, S., and Jendrossek, D. (2018). Determination of Polyhydroxybutyrate (PHB) content in *Ralstonia Eutropha* using gas chromatography and Nile red staining. *Bio-Protocol* 8:e2748. doi: 10.21769/BioProtoc.2748
- Kern, S. E., Price-Whelan, A., and Newman, D. K. (2014). Extraction and measurement of NAD(P)(+) and NAD(P)H. *Methods Mol. Biol.* 1149, 311–323. doi: 10.1007/978-1-4939-0473-0_26
- Koller, M., and Rittmann, S. K. -M. R. (2022). Haloarchaea as emerging big players in future polyhydroxyalkanoate bioproduction: review of trends and perspectives. *Curr. Res. Biotechnol.* 4, 377–391. doi: 10.1016/j.crbiot.2022.09.002
- Lemoigne, M. (1926). Produit de Deshydratation et de Polymerisation de l'acide β -Oxybutyrique. *Bull. Soc. Chim. Biol.* 8, 770–782.
- Letunic, I., and Bork, P. (2021). Interactive tree of life (iTOL) v5: an online tool for phylogenetic tree display and annotation. *Nucleic Acids Res.* 49, W293–W296. doi: 10.1093/nar/gkab301
- Ling, C., Qiao, G.-Q., Shuai, B.-W., Olavarria, K., Yin, J., Xiang, R.-J., et al. (2018). Engineering NADH/NAD⁺ ratio in *Halomonas Bluephagenesis* for enhanced production of Polyhydroxyalkanoates (PHA). *Metab. Eng.* 49, 275–286. doi: 10.1016/j.ymben.2018.09.007
- Markowitz, V. M., Korzeniewski, F., Palaniappan, K., Szeto, E., Werner, G., Padki, A., et al. (2006). The integrated microbial genomes (IMG) system. *Nucleic Acids Res.* 34, D344–D348. doi: 10.1093/nar/gkj024
- Melnik, R. A., Clark, I. C., Liao, A., and Coates, J. D. (2014). Transposon and deletion mutagenesis of genes involved in perchlorate reduction in *Azospira Suillum* PS. *mBio* 5:e00769-13. doi: 10.1128/mBio.00769-13
- Minh, B. Q., Schmidt, H. A., Chernomor, O., Schrempf, D., Woodhams, M. D., von Haeseler, A., et al. (2020). IQ-TREE 2: new models and efficient methods for phylogenetic inference in the genomic era. *Mol. Biol. Evol.* 37, 1530–1534. doi: 10.1093/molbev/msaa015
- Nanninga, H. L., and Gottschal, J. C. (1986). Properties of *Desulfovibrio carbinolicus* sp. nov. and other sulfate-reducing bacteria isolated from an anaerobic-purification plant. *Appl. Environ. Microbiol.* 53, 802–809. doi: 10.1128/aem.53.4.802-809.1987
- Obruca, S., Sedlacek, P., and Koller, M. (2021). The underexplored role of diverse stress factors in microbial biopolymer synthesis. *Bioresour. Technol.* 326:124767. doi: 10.1016/j.biortech.2021.124767
- Page, W. J., and Knosp, O. (1989). Hyperproduction of poly- β -Hydroxybutyrate during exponential growth of *Azotobacter Vinelandii* UWD. *Appl. Environ. Microbiol.* 55, 1334–1339. doi: 10.1128/aem.55.6.1334-1339.1989
- Poli, A., Di Donato, P., Abbamondi, G. R., and Nicolaus, B. (2011). Synthesis, production, and biotechnological applications of exopolysaccharides and polyhydroxyalkanoates by Archaea. *Archaea* 2011, 1–13. doi: 10.1155/2011/693253
- Pötter, M., Müller, H., and Steinbüchel, A. (2005). Influence of homologous Phasins (PhaP) on PHA accumulation and regulation of their expression by the transcriptional repressor PhaR in *Ralstonia Eutropha* H16. *Microbiology* 151, 825–833. doi: 10.1099/mic.0.27613-0
- Redfield, A. C. (1934). "On the proportions of organic derivatives in sea water and their relation to the composition of plankton," in *James Johnson Memorial Volume*, (Liverpool: University of Liverpool), 177–119.
- Rosenboom, J.-G., Langer, R., and Traverso, G. (2022). Bioplastics for a circular economy. *Nature Rev. Materials* 7, 117–137. doi: 10.1038/s41578-021-00407-8
- Sander, K., Abel, A. J., Friedline, S., Sharpless, W., Skerker, J., Deutschbauer, A., et al. (2024). Eliminating genes for a two-component system increases PHB productivity in *Cupriavidus basilensis* 4G11 under PHB suppressing, nonstress conditions. *Biotechnol. Bioeng.* 121, 139–156. doi: 10.1002/bit.28532
- Sayers, E. W., Beck, J., Bolton, E. E., Brister, J. R., Chan, J., Comeau, D. C., et al. (2024). Database resources of the National Center for biotechnology information. *Nucleic Acids Res.* 52, D33–D43. doi: 10.1093/nar/gkad1044
- Scott, F., Yañez, L., Conejeros, R., Araya, B., and Vergara-Fernández, A. (2021). Two internal bottlenecks cause the overflow metabolism leading to poly(3-hydroxybutyrate) production in *Azohydromonas lata* DSM1123. *J. Environ. Chem. Eng.* 9:105665. doi: 10.1016/j.jece.2021.105665
- Senior, P. J., Beech, G. A., RITCHIE, G. A. F., and Dawes, E. A. (1972). The role of oxygen limitation in the formation of poly-P-Hydroxybutyrate during batch and continuous culture of *Azotobacter Beijerinckii*. *Biochem J* 128, 1193–1201. doi: 10.1042/bj1281193
- Steinbüchel, A., and Schlegel, H. G. (1991). Physiology and molecular genetics of poly(β -Hydroxyalkanoic acid) synthesis in *Alcaligenes Eutrophus*. *Mol. Microbiol.* 5, 535–542. doi: 10.1111/j.1365-2958.1991.tb00725.x
- Tang, R., Peng, X., Weng, C., and Han, Y. (2022). The overexpression of Phasin and regulator genes promoting the synthesis of Polyhydroxybutyrate in *Cupriavidus Necator* H16 under nonstress conditions. *Appl. Environ. Microbiol.* 88, e0145821–e0145821. doi: 10.1128/AEM.01458-21
- Wang, L., Liu, Q., Wu, X., Huang, Y., Wise, M. J., Liu, Z., et al. (2019). Bioinformatics analysis of metabolism pathways of archaeal energy reserves. *Sci. Rep.* 9:1034. doi: 10.1038/s41598-018-37768-0
- Williamson, D. H., and Wilkinson, F. (1958). The isolation and estimation of the poly- β -Hydroxy- butyrate inclusions of *Bacillus* species. *J Gen Microbiol* 19, 198–209.
- Wimpenny, J. W. T., and Firth, A. (1972). Levels of nicotinamide adenine dinucleotide and reduced nicotinamide adenine dinucleotide in facultative Bacteria and the effect of oxygen. *J. Bacteriol.* 111, 24–32. doi: 10.1128/jb.111.1.24-32.1972
- Woo, S.-G., Aversch, N. J. H., Berliner, A. J., Deutzmann, J. S., Pane, V. E., Chatterjee, S., et al. (2024). Isolation and characterization of a *Halomonas* species for non-axenic growth-associated production of bio-polyesters from sustainable feedstocks. *Appl. Environ. Microbiol.* 90, e0060324–e0060324. doi: 10.1128/aem.00603-24
- Youngblut, M. D., Wang, O., Barnum, T. P., and Coates, J. D. (2016). (per)chlorate in biology on earth and beyond. *Ann. Rev. Microbiol.* 70, 435–457. doi: 10.1146/annurev-micro-102215-095406
- Zhang, L., Jiang, Z., Tsui, T.-H., Loh, K.-C., Dai, Y., and Tong, Y. W. (2022). A review on enhancing *Cupriavidus necator* fermentation for poly(3-hydroxybutyrate) (PHB) production from low-cost carbon sources. *Front. Bioeng. Biotechnol.* 10:946085. doi: 10.3389/fbioe.2022.946085